

Transverse vortex dynamics in superconductors

J. Lefebvre, M. Hilke,* R. Gagnon, and Z. Altounian

Department of Physics, McGill University, Montréal, Canada H3A 2T8

(Received 19 April 2006; revised manuscript received 24 August 2006; published 15 November 2006)

We experimentally characterize the transverse vortex motion and observe some striking features. We find large structures and peaks in the Hall resistance, which can be attributed to the long-range inhomogeneous vortex flow present in some phases of vortex dynamics. We further demonstrate the existence of a moving vortex phase between the pinned phase (peak effect) and the field induced normal state. The measurements were performed on NiZr₂-based superconducting glasses.

DOI: [10.1103/PhysRevB.74.174509](https://doi.org/10.1103/PhysRevB.74.174509)

PACS number(s): 74.25.Qt, 64.60.Cn, 74.25.Fy, 74.70.Ad

Type II superconductors placed in a magnetic field (B) will allow quantized magnetic fluxes to penetrate and form vortex lines parallel to the field surrounded by superconducting currents. Because of the sign of these currents, single vortices will repel each other and condense at zero temperature into an Abrikosov vortex lattice¹ in the absence of disorder. When introducing disorder and a driving force, the vortex structure will evolve through several different phases, which include a moving Bragg glass, a pinned disordered phase, and a liquidlike phase.²⁻⁴ Theoretically, it is expected that the transverse motion of vortices (perpendicular to the driving force) will also exhibit interesting pinning properties; however, these have been elusive to experiments so far.

To overcome the inherent difficulty in observing the vortex flow at high vortex velocities and densities, where no direct imaging technique can be used, we used dissipative transport in a very clean and isotropic type II superconductor described below. In the mixed state of type II superconductors, the appearance of a resistance is due to the motion of vortices, which upon application of a current (J) in the sample will travel in the direction of the Lorentz force $\vec{J} \times \vec{B}$, thereby inducing a measurable resistance. If the vortices move precisely in the direction of the Lorentz force that is perpendicular to the current direction, no Hall voltage is expected. Therefore, the condition for the onset of a Hall voltage is that the vortices be traveling at some angle to the Lorentz force; then the component of motion parallel to the applied current will induce a Hall voltage. Interestingly, the Hall effect in the superconducting state still eludes the research community; it remains controversial even after over 40 years of research on the subject. Some predict a Hall sign reversal below T_c caused by pinning effects,^{5,6} others argue that the anomaly cannot be due to pinning,⁷⁻¹⁰ while others even predict no sign reversal at all.^{11,12} Moreover, the few studies that report Hall effect measurements on samples which also exhibit the peak effect in longitudinal transport measurements do not show any sharp features^{10,13-15} and no correlation to the different vortex phases was observed.

Many difficulties involved in the analysis of Hall resistance experimental data and theory stem from the competing contributions due to the Hall resistance of normal electrons and the voltage produced by the moving vortices. The contribution to the Hall voltage of the nonsuperconducting or normal electrons can be found in the vortex cores as well as in possible pockets of normal phases in an inhomogeneous

superconductor. In order to circumvent this problem, we have chosen a metallic glass, where the Hall voltage contribution of the normal electrons, antisymmetric in B , is negligible compared to the voltages produced by moving vortices, which is mainly symmetric in B . Indeed, in the normal phase of our system we find $R_H^{\text{asy}} \approx B/ne < 10 \mu\Omega/T$, where $n > 1.4 \times 10^{22} \text{ cm}^{-3}$ is the lower bound for the measured electronic density and R_H^{asy} is always negligible compared to all other contributions. These density values are consistent with those found for melt-spun NiZr₂ ribbons.¹⁶

The measurements of the Hall resistances were performed on glassy Fe_{*x*}Ni_{1-*x*}Zr₂ ribbons for different values of x as a function of magnetic field. The superconducting transition temperature T_c of these high-purity Fe-Ni-Zr based superconducting metal glasses prepared by melt spinning¹⁷ is around 2.3 K depending on the iron content. The amorphous nature of the samples ensures that the pinning is isotropic and has no long-range order, as opposed to crystals, in which long-range order provides strong collective pinning. Also, due to their high purity, the samples have a very weak pinning potential and critical current densities ($J_c \leq 0.4 \text{ A/cm}^2$), a value which is from 10 to 1000 times smaller than in previously studied typical materials.^{8-10,13,15} The advantage of using samples with such a small depinning current resides in the possibility of investigating the pinning and depinning mechanisms of the flux line lattice without the use of a large excitation current, which can introduce uncertainties due to the self-heating it produces. The different length scales characterizing our superconducting samples were estimated from standard expressions for superconductors in the dirty limit,¹⁸ and found to be typical of strong type II low temperature superconductors, as described in Ref. 19.

In the upper panel of Fig. 1, we present a phase diagram obtained from longitudinal resistance measurements for different driving currents I on a sample of Fe_{0.1}Ni_{0.9}Zr₂. The labeling follows the scheme proposed in Ref. 19, where the first depinned vortex phase, labeled depinning 1, is characterized by collectively moving vortices and was identified in Ref. 2 as the moving Bragg glass, in which quasi-long-range order exists. At higher B , the vortices are pinned again (pinning phase); this phase is defined as the peak effect and was proposed to originate from the softening of the vortex lattice,²⁰ which causes the vortex lattice to adapt better to the pinning potential, or from the destruction of long range order by disorder described in the collective pinning theory of

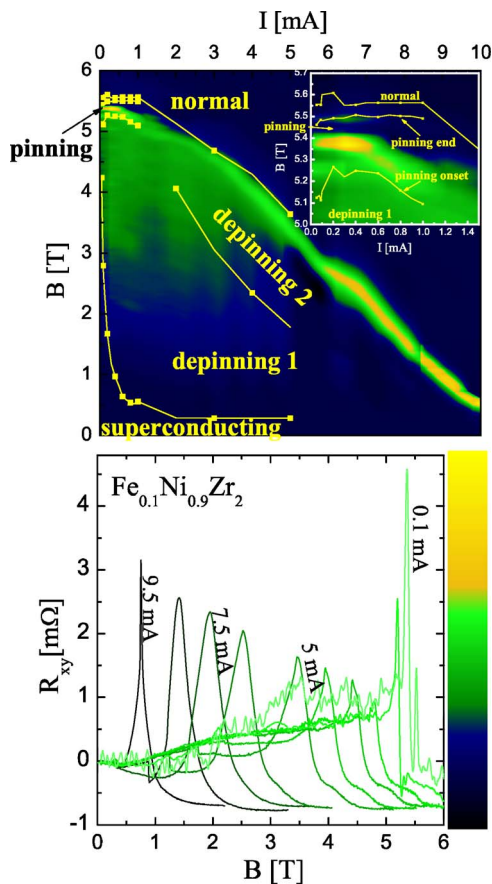


FIG. 1. (Color online) Upper panel: The curves represent the phase diagram obtained from the longitudinal resistance. The color map as a function of B and I represents the value of the Hall resistance according to the color scale shown in the lower panel. It is important to note that a line accounting for the contact misalignment was subtracted from the Hall curves in this graph. The labeling of the different phases is extracted from the longitudinal resistances. Lower panel: Hall resistance as a function of magnetic field for the following driving currents: 0.1, 1, 2.5, 3.33, 4.16, 5, 6.66, 7.5, 8.3, 9.5, and 10 mA.

Larkin and Ovchinnikov.²¹ We have established the onset of the pinning phase as being the point just before the resistance drop where the derivative of R_{xx} vs B is zero. Then the resistance at this point was used as our criteria to determine the end of the pinning phase, i.e., it is determined by taking the point in B after the peak effect where R is the same as at the onset of pinning for each R_{xx} vs B curve. Finally, just below B_{c2} and for higher driving currents, an additional depinned vortex phase is observed (depinning 2), which results from a sudden depinning of the vortex lattice before the transition to the normal state and is characterized by a smectic or plastic flow of vortices.²⁻⁴ The onset of this phase is identified in R_{xx} vs B data as the abrupt increase in resistance following the depinning 1 phase for high driving currents. For low driving currents the nature of the transition between the disordered pinned phase and the normal state was never established, but we show it here to be separated by a depinned phase as evidenced by the existence of a pronounced peak in the Hall resistance.

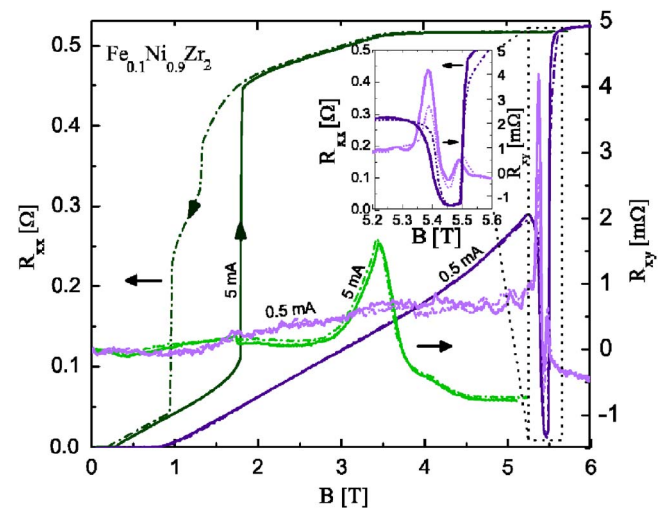


FIG. 2. (Color online) Longitudinal resistance and Hall resistance as a function of magnetic field for up (solid lines) and down (dotted lines) B sweeps with $I=0.5$ mA (purple curves) and $I=5$ mA (green curves). Inset: Enlargement of peak effect region. The experiments were performed in a ^3He system and most of the data presented here was acquired at temperatures around 0.4 K. For the resistance measurements an ac resistance bridge was used at a frequency of 17 Hz. The nonzero Hall resistance above the critical field is due to the small unavoidable misalignment of the Hall contacts.

Also shown in the upper panel of Fig. 1 are the Hall resistances represented as a color map as a function of B and for different driving currents. To ease comparison, the color scale appears in the lower panel of Fig. 1 next to the individual Hall resistance curves. Graphed in this manner the Hall data can be compared directly to the phase diagram and the relation between these two types of measurements is more easily established. Strong peaks or features are observed in the Hall resistance for all driving currents and are found to be located in the depinning 2 phase close to the transition to the normal state in the phase diagram. This can also be observed in Fig. 2, in which Hall resistance curves are plotted with longitudinal resistance curves. Notice that for driving currents below 1 mA a second peak is observed right at the onset of the pinning phase, as can be more easily seen in the inset of Fig. 2, which is just an enlargement of the high B and low I (peak effect) region. The individual Hall resistance curves are shown in the lower panel of Fig. 1, where the peaks observed in the Hall signal are found to vary in amplitude and shape with the driving current.

While we have measured more than half a dozen samples of varying iron concentration, all show very similar features and the results shown in the figures are representative of all. In all the samples there is no single clear-cut distinction between the depinning 1 and 2 phases in terms of the Hall resistance, as opposed to the longitudinal resistance where a jump in the resistance allowed us to determine the boundary. However, the features are always more pronounced in the depinning 2 phase and are highly reproducible for different B sweeps, which stands in contrast to the depinning 1 phase where the smaller features change from sweep to sweep and are indicative of a noisy history dependent behavior. This

behavior of the Hall resistance can be understood in terms of the nature of the different phases. Indeed, in the depinning 1 phase, which is reminiscent of a moving Bragg glass, one would expect a small noisy lateral movement along channels, which depends on the vortex density² and would lead to a noisy B -dependent Hall resistance signal. In the depinning 2 phase, on the other hand, the existence of sharp reproducible peaks in the Hall resistance can be explained by a long range inhomogeneous vortex flow such as that found in smectic channels, where the orientation of the flow can change very suddenly, depending on the local disorder configuration and vortex density. Indeed, the transition from the moving Bragg glass phase to a smectic phase is characterized by a loss of order in the longitudinal direction while long range translational order is maintained in the transverse direction and a decoupling of the channels associated with the insertion of dislocations between the channels. According to Ref. 2, dislocations are created with the increase of disorder (here provided by the B field) or with the increase of the driving force. Generically, a peak in the Hall signal is a measure of a long-ranged moving vortex structure, since a short-ranged order would be averaged out over the sample width, so we expect that the peak observed in the Hall resistance is an indication of a transition to a smectic phase with a reorientation of the vortex flow direction. Finally, in the pinned phase no Hall signal is to be expected as the vortices are immobile, which is indeed what we observe.

A critical reader could argue that the features seen in the Hall resistance are simply due to a long range inhomogeneous current flow as discussed in Ref. 22. Such current distribution could result from parts of the sample becoming normal at a slightly lower magnetic field, as can be expected if the distribution of the Fe content is inhomogeneous in the sample. Fortunately, it is possible to show in our case that most of the signals we measure must come from intrinsic vortex motion. Indeed, using a dc current allows us to separate the different contributions. If the current flow path were to solely determine the Hall voltage, this would imply that $R_H(I, B) \approx R_H(-I, B)$ and $R_H(I, B) \approx R_H(I, -B)$, since the Hall resistance contribution from the normal carriers is negligible. In our samples, however, the differences are almost as large as the values themselves, which therefore excludes a large scale inhomogeneous current flow as the main source for the Hall resistance. A similar argument can be made for intrinsic vortex channels, for which $2R_{\text{odd}}^{\pm} = R_H(I, \pm B) - R_H(-I, \mp B)$ would have to be zero because the electric field due to the vortex flow would be opposite for the paired variables $(I, \pm B)$ and $(-I, \mp B)$ but with the same vortex flow direction. Indeed, the vortex flow direction is antisymmetric in I and B but the electric field produced by the vortex motion is symmetric in B and antisymmetric in I . In general, R_{odd}^+ represents the vortex flow contributions originating from one edge and R_{odd}^- contributions originating from the other edge. If R_{odd} is nonzero, this also implies that the vortex motion cannot be solely described by pure vortex channeling consistent with our measurements that R_{odd} is of the same order as R_H (see Fig. 3). Moreover, it turns out that $R_H^{\text{ac}} \approx R_{\text{even}}^{\pm}$, which is also shown in Fig. 3. This is the reason that most of the data shown here are in fact R_H^{ac} , which is the even contribution of the Hall resistance and represents an average over

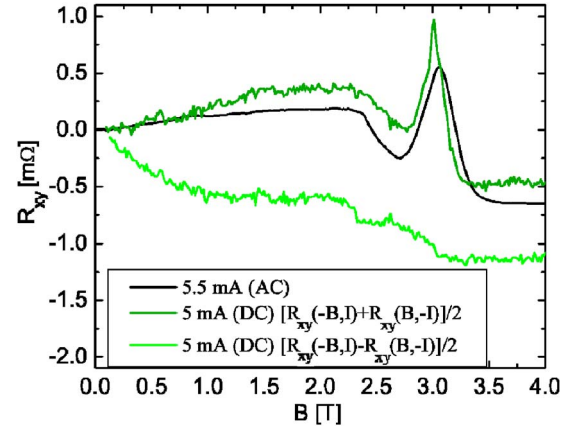


FIG. 3. (Color online) Comparison between the Hall resistance obtained with an ac (17 Hz) excitation current compared to $R_{\text{odd}}^- = [R_{xy}(-B, I) - R_{xy}(B, -I)]/2$ and $R_{\text{even}}^+ = [R_{xy}(-B, I) + R_{xy}(B, -I)]/2$ obtained with dc currents.

vortices flowing in opposite directions, hence avoiding intrinsic edge effects. Finally, this demonstrates that the measured R_H^{ac} is intrinsically due to lateral vortex motion, which cannot come from pure vortex channeling nor inhomogeneous current flow.

We can now analyze the peak effect region of the phase diagram within this framework and show that, indeed, there must exist a moving vortex phase between the pinning phase and the normal state, since we observe a sharp peak in the Hall resistance when sweeping the magnetic field through these regions. Even in the lowest measured currents this peak appears (Fig. 4), suggesting that a different vortex phase with long range inhomogeneous vortex flow such as a smectic phase exists between the peak effect and the normal state all the way down to vanishingly small driving currents. A similar peak is seen in all the samples we have measured and, to the best of our knowledge, this is the first reported evidence for the existence of a smecticlike phase right before the transition to the normal state in such a low driving regime. It is interesting to note that the Hall resistance peak becomes smaller with increasing temperature before vanishing close

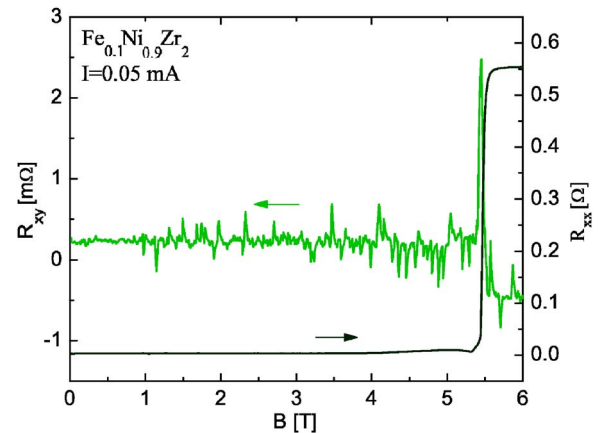


FIG. 4. (Color online) Longitudinal resistance and Hall resistance as a function of magnetic field for B sweeps with $I=0.05$ mA.

to T_c , which further confirms that this peak is not due to an inhomogeneous current flow close to the superconductor to normal transition but rather a consequence of a long-ranged transverse vortex flow just before the critical field.

In summary, we found that in the first depinned vortex phase encountered as the magnetic field is increased, the Hall resistance is relatively smooth with small noisy features, which are a result of some vortices slipping out of the channels in which they flow. This phase is consistent with a moving Bragg glass. At larger magnetic fields, the reentrant pinning phase known as the peak effect, which is characterized by a vanishing longitudinal resistance, also leads to a zero Hall resistance. More interestingly, at even higher fields and

for all driving currents, large features and peaks are observed in the Hall resistance in the second depinning phase close to the normal state. These important features are characteristic of a long range inhomogeneous vortex flow, such as expected in a smectic phase with orientational changes. Also important is the strong peak feature observed, even at low driving currents, between the disordered pinned phase and the normal state, which demonstrates the existence of a long range moving vortex phase in that region.

The authors acknowledge support from FQRNT and NSERC.

*Author to whom correspondence should be addressed. Electronic address: hilke@physics.mcgill.ca

- ¹A. A. Abrikosov, *Sov. Phys. JETP* **5**, 1174 (1957).
- ²P. Le Doussal and T. Giamarchi, *Phys. Rev. B* **57**, 11356 (1998).
- ³C. J. Olson, C. Reichhardt, and F. Nori, *Phys. Rev. Lett.* **81**, 3757 (1998).
- ⁴H. Fangohr, S. J. Cox, and P. A. J. de Groot, *Phys. Rev. B* **64**, 064505 (2001).
- ⁵Z. D. Wang and C. S. Ting, *Phys. Rev. Lett.* **67**, 3618 (1991).
- ⁶B. Y. Zhu, D. Y. Xing, Z. D. Wang, B. R. Zhao, and Z. X. Zhao, *Phys. Rev. B* **60**, 3080 (1999).
- ⁷V. M. Vinokur, V. B. Geshkenbein, M. V. Feigel'man, and G. Blatter, *Phys. Rev. Lett.* **71**, 1242 (1993).
- ⁸S. J. Hagen, C. J. Lobb, R. L. Greene, M. G. Forrester, and J. H. Kang, *Phys. Rev. B* **41**, 11630 (1990).
- ⁹C. J. Lobb, T. Clinton, A. P. Smith, P. Liu, P. Li, J. L. Peng, R. L. Greene, M. Eddp, and C. C. Tsuei, *Appl. Supercond.* **2**, 631 (1994).
- ¹⁰S. Bhattacharya, M. J. Higgins, and T. V. Ramakrishnan, *Phys. Rev. Lett.* **73**, 1699 (1994).
- ¹¹J. Bardeen and M. Stephen, *Phys. Rev.* **140**, A1197 (1964).
- ¹²A. I. Schindler and D. J. Gillespie, *Phys. Rev.* **130**, 953 (1963).
- ¹³T. W. Jing and N. P. Ong, *Phys. Rev. B* **42**, 10781 (1990).
- ¹⁴A. K. Niessen and F. A. Staas, *Phys. Lett.* **15**, 26 (1965).
- ¹⁵A. Niessen and C. Weijnsfeld, *J. Appl. Phys.* **40**, 384 (1969).
- ¹⁶R. W. Cochrane, J. Destry, and M. Trudeau, *Phys. Rev. B* **27**, 5955 (1983).
- ¹⁷Z. Altounian, S. V. Dantu, and M. Dikeakos, *Phys. Rev. B* **49**, 8621 (1994).
- ¹⁸P. H. Kes and C. C. Tsuei, *Phys. Rev. B* **28**, 5126 (1983).
- ¹⁹M. Hilke, S. Reid, R. Gagnon, and Z. Altounian, *Phys. Rev. Lett.* **91**, 127004 (2003).
- ²⁰A. B. Pippard, *Proc. R. Soc. London, Ser. A* **216**, 547 (1953).
- ²¹A. I. Larkin and Y. N. Ovchinnikov, *Sov. Phys. JETP* **41**, 960 (1975).
- ²²G. Doornbos, R. Wijngaarden, and R. Griessen, *Physica C* **235-240**, 1371 (1994).